The current issue and full text archive of this journal is available at
www.emeraldinsight.com/0961-5539.htm

Mixed convection heat and mass transfer of non-Newtonian fluids from a permeable surface embedded in a porous medium

Ali J. Chamkha
Manufacturing Engineering Department, The Public Authority for Applied Education and Training, Shuweikh, Kuwait, and
Jasem M. Al-Humoud
Civil Engineering Department, Kuwait University, Safat, Kuwait

Abstract

Purpose – To consider simultaneous heat and mass transfer by mixed convection for a non-Newtonian power-law fluid from a permeable vertical plate embedded in a fluid-saturated porous medium in the presence of suction or injection and heat generation or absorption effects.

Design/methodology/approach – The problem is formulated in terms of non-similar equations. These equations are solved numerically by an efficient implicit, iterative, finite-difference method.

Findings – It was found that as the buoyancy ratio was increased, both the local Nusselt and Sherwood numbers increased in the whole range of free and mixed convection regime while they remained constant for the forced-convection regime. However, they decreased and then increased forming dips as the mixed-convection parameter was increased from the free-convection limit to the forced-convection limit for both Newtonian and dilatant fluid situations.

Research limitations/implications – The problem is limited to slow flow of non-Newtonian power-law fluids in porous media. Future research may consider inertia effects of porous media for relatively higher velocity flows.

Practical implications – A very useful source of information for researchers on the subject of non-Newtonian fluids in porous media.

Originality/value – This paper illustrates simultaneous heat and mass transfer in porous media for power-law fluids with heat generation or absorption effects.

Keywords Convection, Porosity, Flow, Heat transfer, Numerical analysis

Paper type Research paper

Nomenclature

C = dimensionless concentration, $C = (c - c_\infty)/(c_w - c_\infty)$
c = concentration at any point in the flow field
c_p = specific heat at constant pressure
c_∞ = concentration at the free stream
c_w = concentration at the wall
D = mass diffusivity
d = particle diameter of the porous medium
f = dimensionless stream function $f = \psi/\left[\alpha_e(Pe_x^{1/2} + Ra_x^{1/2})\right]$
g = gravitational acceleration
h = local convective heat transfer coefficient
h_m = local mass transfer coefficient
K = modified permeability of the porous medium
k_e = porous medium effective thermal conductivity

International Journal of Numerical Methods for Heat & Fluid Flow
Vol. 17 No. 2, 2007
pp. 195-212
© Emerald Group Publishing Limited
0961-5539
DOI 10.1108/09615530710723966

Le = Lewis number, $Le = \alpha_e/D$
N = buoyancy ratio, $N = \beta_c(c_w - c_\infty)/[\beta_T(T_w - T_\infty)]$
Nu_x = local Nusselt number, $Nu_x = hx/k_e$
Pe_x = local Peclet number, $Pe_x = U_\infty x/\alpha_e$
Q_o = heat generation or absorption coefficient
Ra_x = local Rayleigh number, $Ra_x = x/\alpha_e[\rho g \beta_T | T_w - T_\infty | K/\mu]^{1/n}$
Sh_x = local Sherwood number, $Sh_x = h_m x/D$
T = temperature at any point
T_w = wall temperature
T_∞ = free stream temperature
u = tangential or x-component of velocity
v = normal or y-component of velocity
v_o = suction or injection velocity
U_∞ = free stream velocity
x = distance along the surface
y = distance normal to the surface

Greek symbols

α_e = effective thermal diffusivity of the porous medium
β_c = concentration expansion coefficient
β_T = thermal expansion coefficient
ε = porosity of the porous medium
ϕ = dimensionless heat generation or absorption parameter, $\phi = Q_o/(\rho c_p v_o)$
η = coordinate transformation in terms of x and y, $\eta = y(Pe_x^{1/2} + Ra_x^{1/2})/x$
χ = mixed convection parameter, $\chi = [1 + (Ra_x/Pe_x)^{1/2}]^{-1}$
ψ = stream function
θ = dimensionless temperature, $\theta = (T - T_\infty)/(T_w - T_\infty)$
ρ = fluid density
ξ = transformed suction or injection parameter, $\xi = v_o x(Pe_x^{1/2} + Ra_x^{1/2})^{-1}/\alpha_e$

Introduction

Buoyancy-induced flows from vertical surfaces embedded in porous media have been the subject of many investigations. This is due fact that these flows have many engineering and geophysical applications such as geothermal reservoirs, drying of porous solids, thermal insulation, enhanced oil recovery, groundwater pollution, and underground energy transport. Cheng and Minkowycz (1977) have presented similarity solutions for free thermal convection from a vertical plate in a fluid-saturated porous medium. Ranganathan and Viskanta (1984) have considered mixed convection boundary layer flow along a vertical surface in a porous medium. Nakayama and Koyama (1987) have suggested similarity transformations for pure, combined and forced convection in Darcian and non-Darcian porous media. Lai (1991) has investigated coupled heat and mass transfer by mixed convection from an isothermal vertical plate in a porous medium. Hsieh *et al.* (1993) have presented non-similar solutions for combined convection in porous media. All of the above references considered Newtonian fluids.

A number of industrially important fluids such as molten plastics, polymers, pulps, foods and slurries and fossil fuels which may saturate underground beds display non-Newtonian power-law fluid behavior. Non-Newtonian fluids exhibit a non-linear relationship between shear stress and shear rate. An illustrative example of non-Newtonian power-law fluid flow in porous medium is found in oil reservoir engineering in connection with the production of heavy crude oils. This process involves periodic injection of steam or placement of heat generation sources for the purpose of increasing the crude oil temperature. The increase in crude oil temperature reduces its viscosity and thus, enhances its mobility resulting in improved oil production flow rates. Chen and Chen (1988) have presented similarity solutions for free convection of non-Newtonian fluids over vertical surfaces in porous media. Mehta

and Rao (1994a) have investigated buoyancy-induced flow of non-Newtonian fluids over a non-isothermal horizontal plate embedded in a porous medium. Also, Mehta and Rao (1994b) have analyzed buoyancy-induced flow of non-Newtonian fluids in a porous medium past a vertical plate with non-uniform surface heat flux. In a series of papers, Gorla and co-workers (Gorla *et al.*, 1997a, b, 1998; Kumari *et al.*, 1997; Gorla and Kumari, 1998) have studied mixed convection in non-Newtonian fluids along horizontal and vertical plates in porous media. Jumah and Mujumdar (2000) have considered free convection heat and mass transfer of non-Newtonian power-law fluids with yield stress from a vertical flat plate in saturated porous media.

In certain porous media applications such as those involving heat removal from nuclear fuel debris, underground disposal of radioactive waste material, storage of food stuffs, and exothermic chemical reactions and dissociating fluids in packed-bed reactors, the working fluid heat generation or absorption effects are important. Modeling of such situations involves the addition of a heat source or sink term in the energy equation. This term has been assumed to be either a constant (Acharya and Goldstein, 1985) or temperature-dependent (Vajravelu and Nayfeh, 1992).

The effects of fluid wall suction or injection the flow and heat transfer characteristics along vertical semi-infinite plates have been investigated by several authors (Cheng, 1977; Lai and Kulacki, 1990a, b; Minkowycz *et al.*, 1985; Hooper *et al.*, 1993). Some of these studies have reported similarity solutions (Cheng, 1977; Lai and Kulacki, 1990a, b) while others have obtained non-similar solutions (Minkowycz *et al.*, 1985; Hooper *et al.*, 1993). Lai and Kulacki (1990a, b) have reported similarity solutions for mixed convection flow over horizontal and inclined plates embedded in fluid-saturated porous media in the presence of surface mass flux. On the other hand, Minkowycz *et al.* (1985) have discussed the effect of surface mass transfer on buoyancy-induced Darcian flow adjacent to a horizontal surface using non-similarity solutions. Also, Hooper *et al.* (1993) have considered the problem of non-similar mixed convection flow along an isothermal vertical plate in porous media with uniform surface suction or injection and introduced a single parameter for the entire regime of free-forced-mixed convection. Their non-similar variable represented the effect of suction or injection at the wall.

The objective of this paper is consider simultaneous heat and mass transfer by mixed convection for a non-Newtonian power-law fluid from a permeable vertical plate embedded in a fluid-saturated porous medium in the presence of suction or injection and heat generation or absorption effects. This will be done for constant temperature and concentration wall conditions in the entire range of free-forced-mixed convection regime.

Problem formulation

Consider steady mixed convection flow of a non-Newtonian power-law fluid over a permeable semi-infinite vertical surface embedded in a porous medium in the presence of temperature difference-dependent heat generation or absorption. The power-law fluid model of Ostwald-de-Waele which is adequate for many non-Newtonian fluids is considered herein. Uniform suction or injection with speed v_o is imposed at the surface boundary. The porous medium is assumed to be uniform, isotropic and in thermal equilibrium with the fluid. All fluid properties are assumed constant. Under the

Boussinesq and boundary-layer approximations, the governing equations for this problem can be written as:

$$\frac{\partial u}{\partial x}+\frac{\partial v}{\partial y}=0 \tag{1}$$

$$u^n = U_\infty^n + \frac{K}{\mu}\rho g[\beta_{\mathrm{T}}(T-T_\infty)+\beta_{\mathrm{c}}(c-c_\infty)] \tag{2}$$

$$u\frac{\partial T}{\partial x}+v\frac{\partial T}{\partial y}=\alpha_{\mathrm{e}}\frac{\partial^2 T}{\partial y^2}+\frac{Q_o}{\rho c_{\mathrm{p}}}(T-T_\infty) \tag{3}$$

$$u\frac{\partial c}{\partial x}+v\frac{\partial c}{\partial y}=D\frac{\partial^2 c}{\partial y^2} \tag{4}$$

where x and y denote the vertical and horizontal directions, respectively. u, v, T and c are the x- and y-components of velocity, temperature and concentration, respectively. ρ, μ, n, c_{p} and D are the fluid density, consistency index for viscosity, power-law fluid viscosity index, specific heat at constant pressure, and mass diffusion coefficient, respectively. K and α_{e} are the porous medium permeability and effective thermal diffusivity, respectively. β_{T}, β_{c}, Q_o, U_∞, T_∞ and c_∞ are the thermal expansion coefficient, concentration expansion coefficient, heat generation (>0) or absorption (<0) coefficient and the free stream velocity, temperature and concentration, respectively.

The modified permeability of the porous medium K for flows of non-Newtonian power-law fluids is given by:

$$K=\frac{1}{2C_t}\left(\frac{n\varepsilon}{3n+1}\right)^n\left(\frac{50k^*}{3\varepsilon}\right)^{(n+1)/2} \tag{5}$$

where

$$k^* = \frac{\varepsilon^3 d^2}{150(1-\varepsilon)^2} \tag{6}$$

$$C_t=\begin{cases}\dfrac{25}{12}\\[2ex] \dfrac{2}{3}\left(\dfrac{8n}{9n+3}\right)\left(\dfrac{10n-3}{6n+1}\right)\left(\dfrac{75}{16}\right)^{3(10n-3)/(10n+11)}\end{cases} \tag{7}$$

(Christopher and Middleman, 1965; Dharmadhikari and Kale, 1985) where ε and d is the porosity and the particle diameter of the porous medium.

The boundary conditions suggested by the physics of the problem are:

$$\begin{gathered} v(x,0)=v_o,\ T(x,0)=T_{\mathrm{w}},\ c(x,0)=c_{\mathrm{w}} \\ u(x,\infty)=U_\infty,\ T(x,\infty)=T_\infty,\ c(x,\infty)=c_\infty \end{gathered} \tag{8}$$

where T_{w} and c_{w} are the wall temperature and concentration, respectively.

It is convenient to transform the governing equations into a non-similar dimensionless form which can be suitable for solution as an initial-value problem. This can be done by introducing the stream function such that:

$$u = \frac{\partial \psi}{\partial y}, v = -\frac{\partial \psi}{\partial x} \tag{9}$$

and using

$$\eta = \frac{y}{x}\left(Pe_x^{1/2} + Ra_x^{1/2}\right), \quad \xi = \frac{v_o x}{\alpha_e}\left(Pe_x^{1/2} + Ra_x^{1/2}\right)^{-1} \tag{10}$$

$$\psi = \alpha_e\left(Pe_x^{1/2} + Ra_x^{1/2}\right) f(\xi, \eta), \quad \theta(\xi, \eta) = \frac{T - T_\infty}{T_w - T_\infty}, \quad C(\xi, \eta) = \frac{c - c_\infty}{c_w - c_\infty} \tag{11}$$

where $Pe_x = U_\infty x/\alpha_e$ and $Ra_x = x/\alpha_e[\rho g \beta_T |T_w - T_\infty| K/\mu]^{1/n}$ are the local Peclet and modified Rayleigh numbers, respectively.

Substituting equations (9) through (11) into equations (1) through (5) produces:

$$nf'^{n-1}f'' = (1 - \chi)^{2n}(\theta' + NC') \tag{12}$$

$$\theta'' + \frac{1}{2}f\theta' + \xi^2\phi\theta = \frac{1}{2}\xi\left(f'\frac{\partial \theta}{\partial \xi} - \theta'\frac{\partial f}{\partial \xi}\right) \tag{13}$$

$$Le^{-1}C'' + \frac{1}{2}fC' = \frac{1}{2}\xi\left(f'\frac{\partial C}{\partial \xi} - C'\frac{\partial f}{\partial \xi}\right) \tag{14}$$

$$\begin{gathered} f(\xi, 0) + \xi\frac{\partial f}{\partial \xi}(\xi, 0) = -2\xi, \theta(\xi, 0) = 1, C(\xi, 0) = 1 \\ f(\xi, \infty) = \chi^2, \theta(\xi, \infty) = 0, C(\xi, \infty) = 0 \end{gathered} \tag{15}$$

where

$$Le = \frac{\alpha_e}{D}, \quad N = \frac{\beta_c(c_w - c_\infty)}{\beta_T(T_w - T_\infty)}, \quad \phi = \frac{Q_o}{\rho c_p v_o}, \quad \chi = \left[1 + \left(\frac{Ra_x}{Pe_x}\right)^{1/2}\right]^{-1} \tag{16}$$

are the Lewis number, concentration to thermal buoyancy ratio, dimensionless heat generation (>0) or absorption (<0) coefficient, and the mixed convection parameter, respectively. It should be noted that $\chi = 0$ ($Pe_x = 0$) corresponds to pure free convection while $\chi = 1$ ($Ra_x = 0$) corresponds to pure forced convection. The entire regime of mixed convection corresponds to values of χ between 0 and 1.

Of special significance for this problem are the local Nusselt and Sherwood numbers. These physical quantities can be defined as:

$$Nu_x = \frac{hx}{k_e} = -\left(Pe_x^{1/2} + Ra_x^{1/2}\right)\theta'(\xi, 0); \quad h = \frac{q_w}{T_w - T_\infty}; \quad q_w = -k_e\left(\frac{\partial T}{\partial y}\right)_{y=0} \tag{17}$$

$$Sh_x = \frac{h_m x}{D} = -\left(Pe_x^{1/2} + Ra_x^{1/2}\right) C'(\xi, 0); \quad h_m = \frac{m_w}{c_w - c_\infty}; \quad m_w = -D\left(\frac{\partial c}{\partial y}\right)_{y=0} \tag{18}$$

where k_e is the porous medium effective thermal conductivity and q_w and m_w are, respectively, the wall heat transfer and wall mass transfer.

Numerical method and validation

Equations (15) through (18) represent an initial-value problem with ξ playing the role of time. This non-linear problem cannot be solved in closed form and, therefore, a numerical solution is necessary to describe the physics of the problem. The implicit, tri-diagonal finite-difference method similar to that discussed by Blottner (1970) has proven to be adequate and sufficiently accurate for the solution of this kind of problems. Therefore, it is adopted in the present work.

All first-order derivatives with respect to ξ are replaced by two-point backward-difference formulae when marching in the positive ξ direction and by two-point forward-difference formulae when marching in the negative ξ direction. Then, all second-order differential equations in η are discretized using three-point central difference quotients. This discretization process produces a tri-diagonal set of algebraic equations at each line of constant ξ which is readily solved by the well known Thomas algorithm (Blottner, 1970). During the solution, iteration is employed to deal with the non-linearities of the governing differential equations. The problem is solved line by line starting with line $\xi = 0$ where similarity equations are solved to obtain the initial profiles of velocity, temperature and concentration and marching forward (or backward) in ξ until the desired line of constant ξ is reached. Variable step sizes in the η direction with $\Delta\eta_1 = 0.001$ and a growth factor $G = 1.04$ such that $\Delta\eta_n = G\Delta\eta_{n-1}$ and constant step sizes in the ξ direction with $\Delta\xi = 0.01$ are employed. These step sizes are arrived at after many numerical experimentations performed to assess grid independence. The convergence criterion employed in the present work is based on the difference between the current and the previous iterations. When this difference reached 10^{-6} for all points in the η directions, the solution was assumed converged and the iteration process was terminated.

Tables I and II present a comparison of $-\theta'(\xi, 0)$ at selected values of ξ and χ between the results of the present work and those reported earlier by Hooper *et al.* (1993) for $n = 1$, $N = 0$ and $\phi = 0$. It is clear from this comparison that a good

χ	$\xi = -2.0$	$\xi = -1.5$	$\xi = -1.0$	$\xi = -0.5$	$\xi = 0.0$	$\xi = 0.5$	$\xi = 1.0$	$\xi = 1.5$	$\xi = 2.0$
0.0	1.9989	1.5135	1.0726	0.7121	0.4440	0.2601	0.1424	0.0725	0.0341
0.1	1.9979	1.5060	1.0509	0.6770	0.4037	0.2230	0.1134	0.0526	0.0221
0.2	1.9976	1.5027	1.0383	0.6526	0.3734	0.1944	0.0914	0.0384	0.0143
0.3	1.9975	1.5020	1.0340	0.6406	0.3552	0.1757	0.0769	0.0294	0.0097
0.4	1.9976	1.5635	1.0373	0.6415	0.3507	0.1681	0.0700	0.0250	0.0075
0.5	1.9982	1.5050	1.0478	0.6545	0.3605	0.1725	0.0710	0.0248	0.0073
0.6	2.0006	1.5165	1.0653	0.6783	0.3834	0.1890	0.0803	0.0240	0.0088
0.7	2.0058	1.5298	1.0895	0.7112	0.4175	0.2167	0.0982	0.0385	0.0129
0.8	2.0148	1.5485	1.1202	0.7515	0.4604	0.2539	0.1247	0.0541	0.0206
0.9	2.0283	1.5728	1.1568	0.7978	0.5100	0.2986	0.1590	0.0764	0.0329
1.0	2.0497	1.6025	1.1990	0.8488	0.5643	0.3483	0.1998	0.1049	0.0504

Table I.
Values of $-\theta'(\xi, 0)$ at selected values of ξ and χ for $n = 1$, $N = 0$ and $\phi = 0$ (present work)

χ	$\xi = -2.0$	$\xi = -1.5$	$\xi = -1.0$	$\xi = -0.5$	$\xi = 0$	$\xi = 0.5$	$\xi = 1.0$	$\xi = 1.5$	$\xi = 2.0$
0.0	2.0015	1.5148	1.0725	0.7114	0.4437	0.2593	0.1417	0.0717	0.0335
0.1	2.0005	1.5076	1.0510	0.6763	0.4035	0.2223	0.1127	0.0519	0.0216
0.2	2.0003	1.5046	1.0386	0.6520	0.3732	0.1937	0.0907	0.0378	0.0139
0.3	2.0003	1.5042	1.0347	0.6401	0.3550	0.1750	0.0762	0.0288	0.0084
0.4	2.0005	1.5060	1.0384	0.6411	0.3504	0.1674	0.0693	0.0244	0.0072
0.5	2.0016	1.5106	1.0491	0.6543	0.3603	0.1719	0.0704	0.0242	0.0069
0.6	2.0042	1.5192	1.0666	0.6782	0.3832	0.1884	0.0797	0.0284	0.0085
0.7	2.0095	1.5324	1.0908	0.7111	0.4196	0.2036	0.0999	0.0339	0.0134
0.8	2.0185	1.5510	1.1214	0.7515	0.4602	0.2534	0.1242	0.0535	0.0201
0.9	2.0319	1.5751	1.1579	0.7978	0.5097	0.2982	0.1586	0.0758	0.0324
1.0	1.0502	1.6047	1.1995	0.8488	0.5642	0.3488	0.1996	0.1047	0.0502

Source: Hooper *et al.* (1993)

Table II.
Values of $-\theta'(\xi, 0)$ at selected values of ξ and χ for $n = 1$, $N = 0$ and $\phi = 0$

agreement between the results exists. This lends confidence in the correctness of the numerical results to be reported subsequently. It should be noted that in Table II, the value of $-\theta'(\xi, 0)$ at $\xi = -2$ and $\chi = 1$ seems to be in error or a typo as this value cannot be 1.0502.

Results and discussion

Figures 1-3 show representative velocity, temperature and concentration (f', θ and C) profiles for different values of the transformed suction or injection parameter ξ and two distinct values of the buoyancy ratio $N = 0$, 3 and power-law fluid index $n = 0.5$ (shear thinning or pseudo-plastic fluid), respectively. For a fixed value of $\chi = 0.5$ ($Ra_x/Pe_x = 1$) increases in the value of N has the tendency to increase the buoyancy

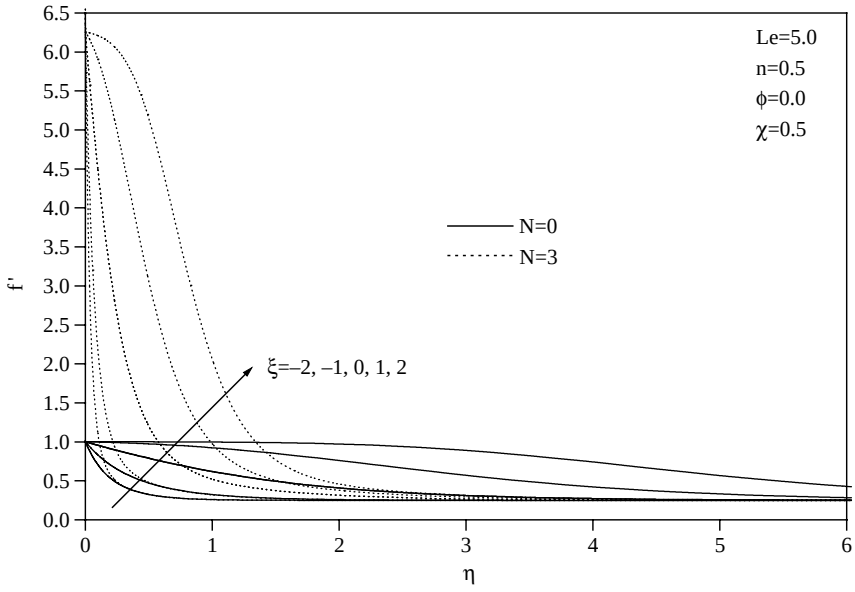

Figure 1.
Velocity profiles for different values of ξ ($n = 0.5$)

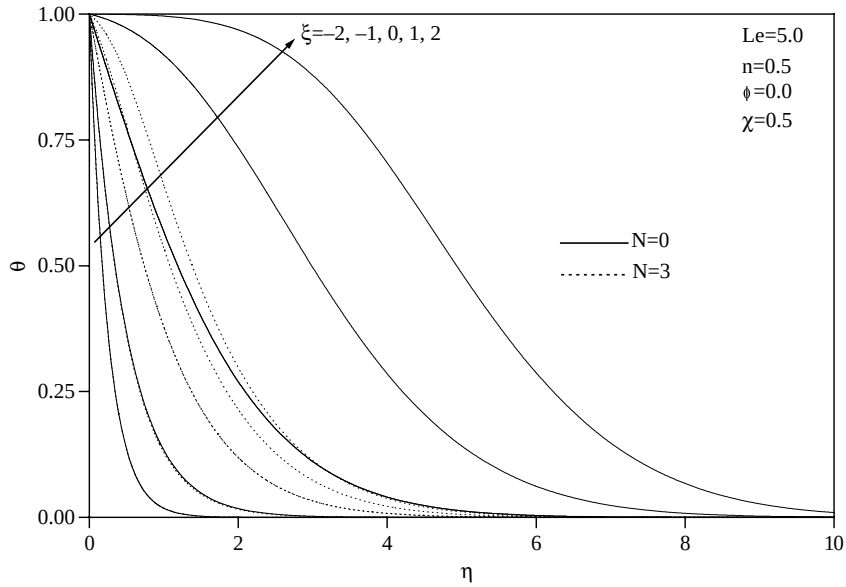

Figure 2.
Temperature profiles for different values of ξ ($n = 0.5$)

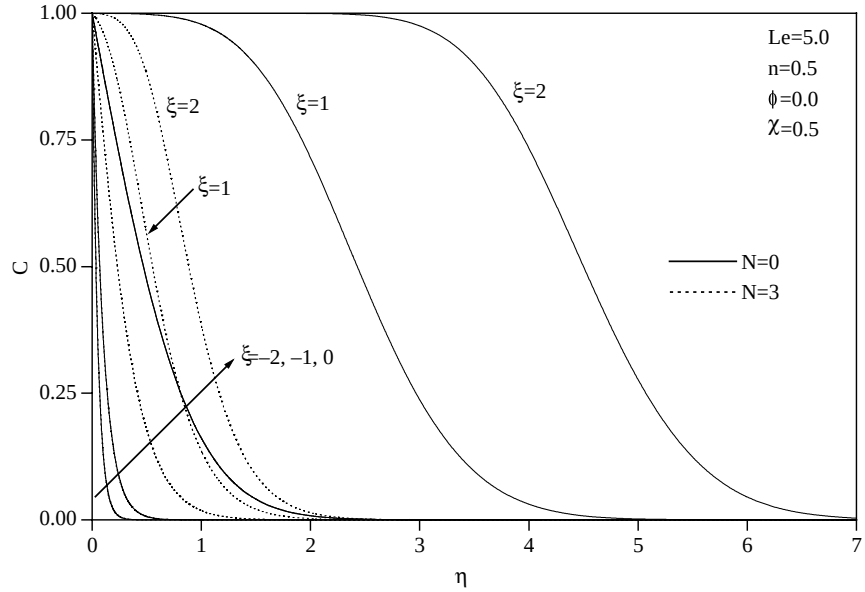

Figure 3.
Concentration profiles for different values of ξ ($n = 0.5$)

effect causing more induced flow along the plate in the vertical direction. This enhancement in the flow velocity is achieved at the expense of reduced fluid temperature and concentration as well as reduced thermal and concentration boundary layers as seen from Figures 2 and 3. Also, as ξ increases, all of the velocity, temperature and concentration along with their boundary layers are predicted to increase.

Similar results as those shown in Figures 1-3 are shown in Figures 4-6 but for $n = 1.5$ (shear thickening or dilatant fluid). The effects of increasing N and ξ are the same as discussed above for $n = 0.5$. Comparison of Figures 1-3 with Figures 4-6 shows that as n increases, the fluid velocity decreases while the temperature and

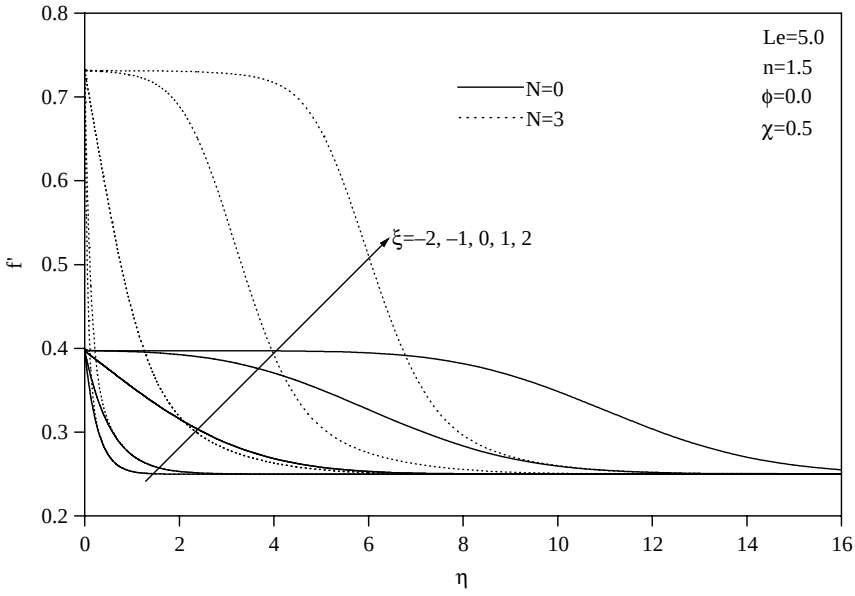

Figure 4.
Velocity profiles for different values of ξ ($n = 1.5$)

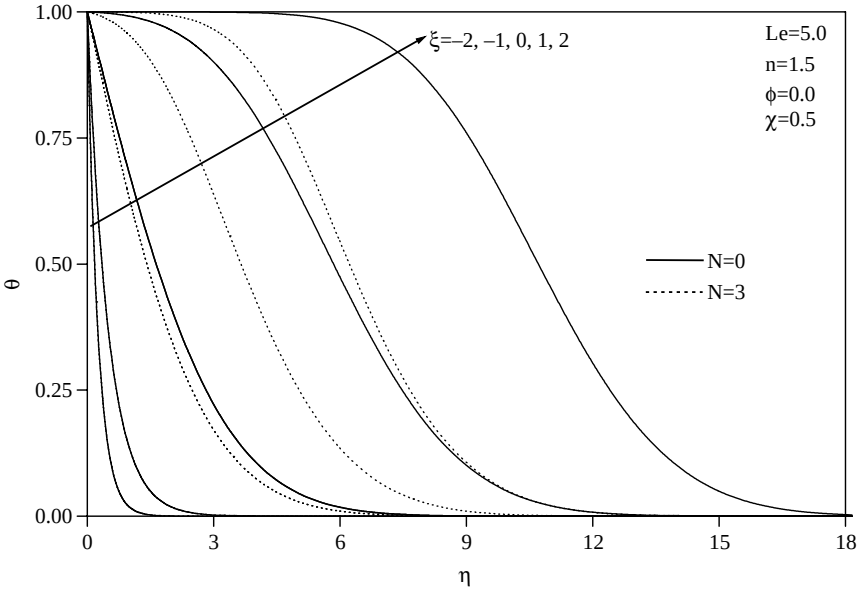

Figure 5.
Temperature profiles for different values of ξ ($n = 1.5$)

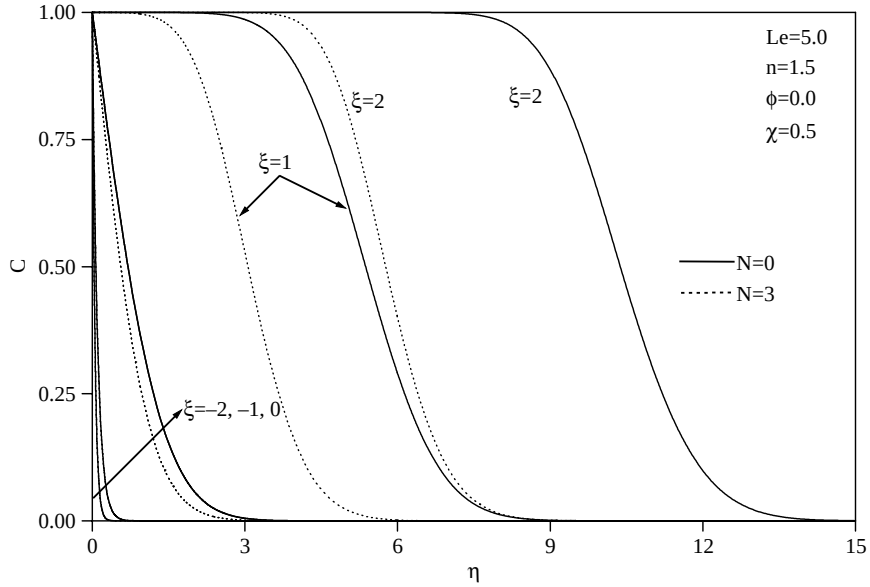

Figure 6.
Concentration profiles for different values of ξ ($n = 1.5$)

concentration and their boundary layers increase. Furthermore, inspection of Figures 1-6 shows that while the changes in the profiles corresponding to $\xi = 0$, $\xi = 1$ and $\xi = 2$ as N increases are significant, they are insignificant for the profiles corresponding to $\xi = -1$ and $\xi = -2$.

Figures 7-12 show the effects of the buoyancy ratio N and the transformed suction or injection parameter ξ in the range of the mixed convection parameter $0 \leq \chi \leq 1$ on

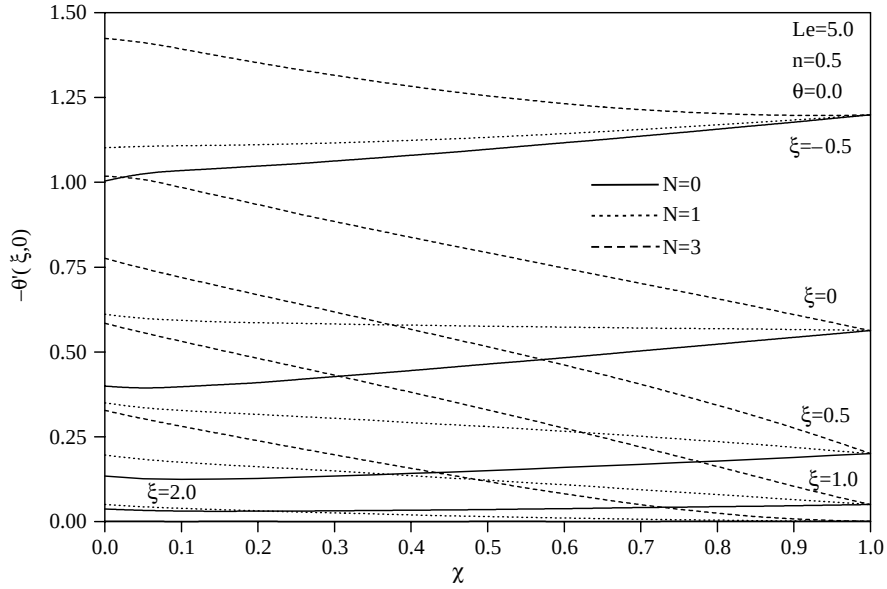

Figure 7.
Effects of N and χ on local Nusselt number for $n = 0.5$ and different ξ values

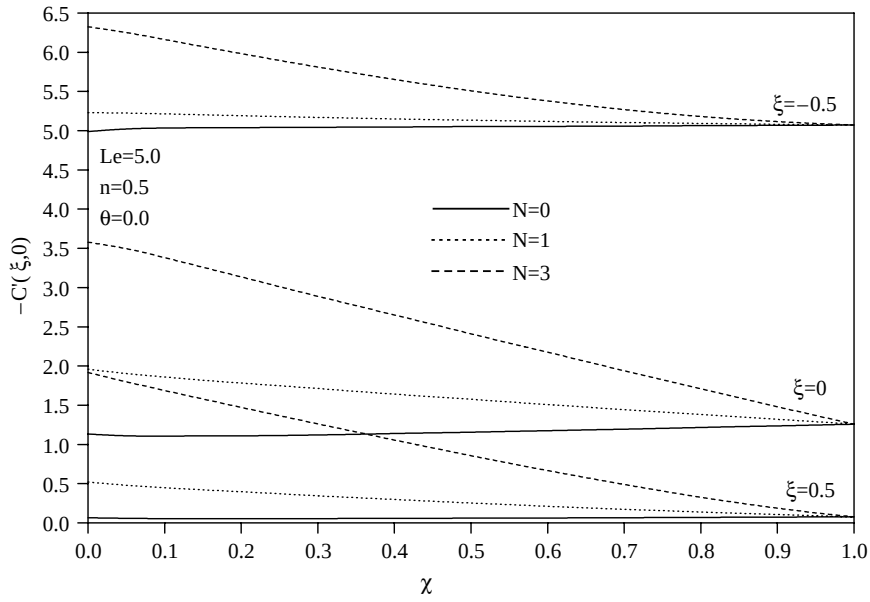

Figure 8.
Effects of N and χ on local Sherwood number for $n = 0.5$ and different ξ values

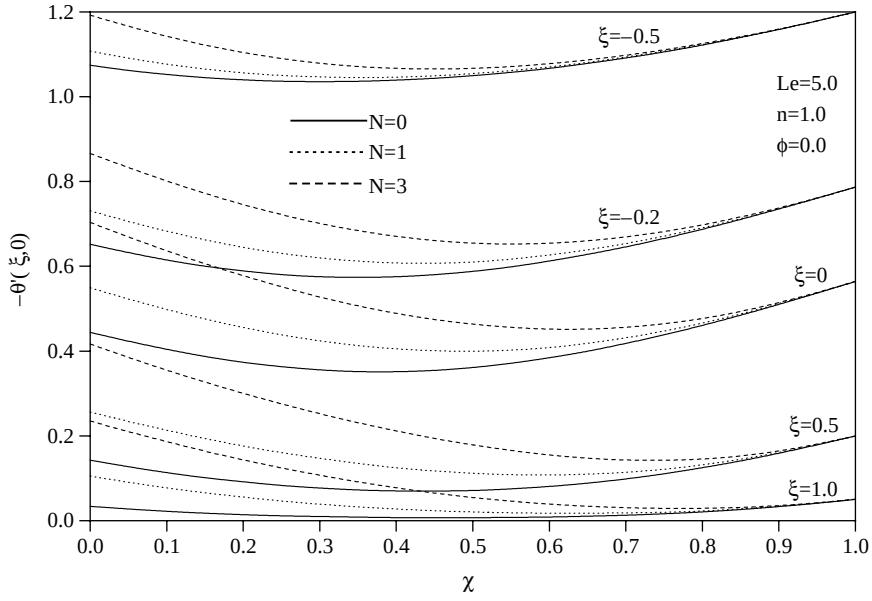

Figure 9.
Effects of N and χ on local Nusselt number for $n = 1.0$ and different ξ values

the local Nusselt number $[Nu_x/(Pe_x^{1/2} + Ra_x^{1/2}) = -\theta'(\xi, 0)]$ and the local Sherwood number $[Sh_x/(Pe_x^{1/2} + Ra_x^{1/2}) = -C'(\xi, 0)]$ for power-law fluid viscosity indices $n = 0.5$ (shear-thinning or pseudo-plastic fluid), $n = 1.0$ (Newtonian fluid) and $n = 1.5$ (shear-thickening or dilatant fluid), respectively. As mentioned before, in general,

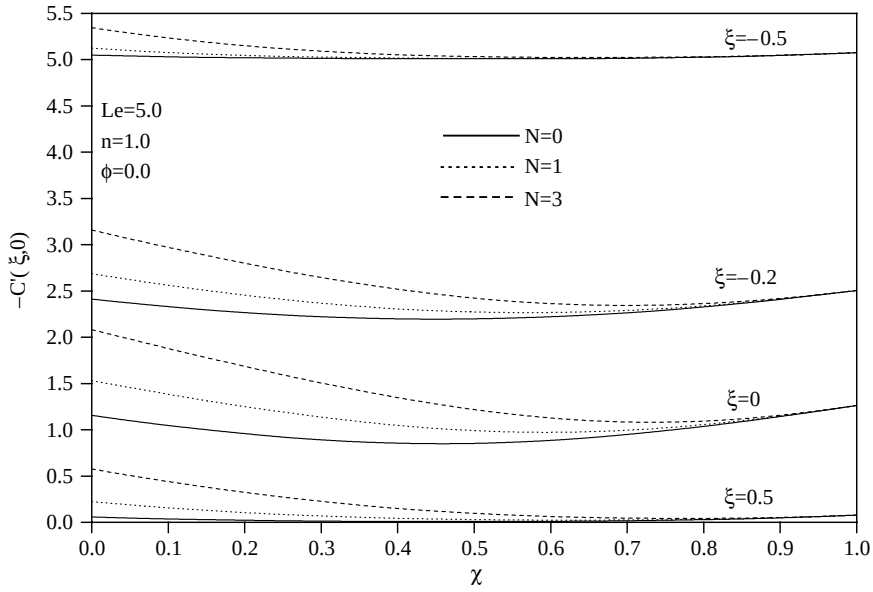

Figure 10.
Effects of N and χ on local Sherwood number for $n = 1.0$ and different ξ values

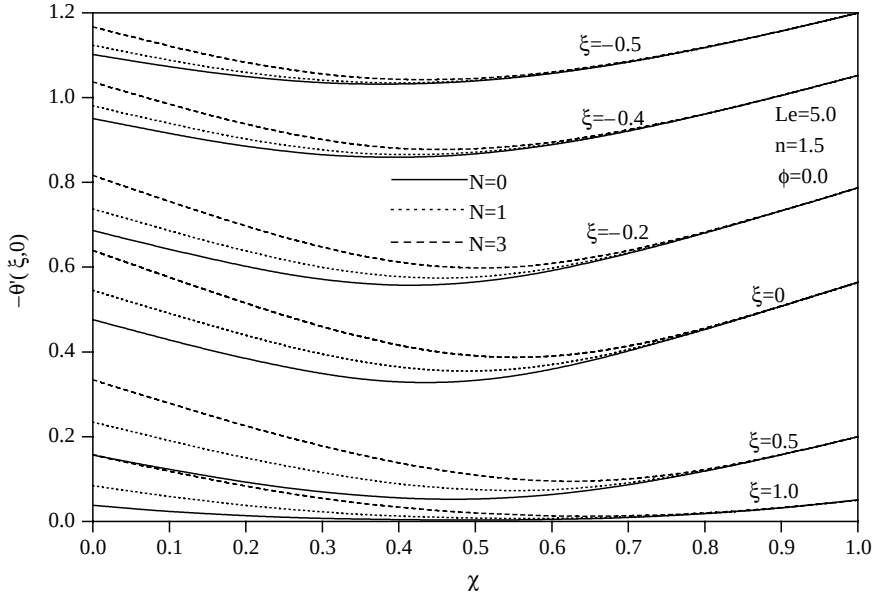

Figure 11.
Effects of N and χ on local Nusselt number for $n = 1.5$ and different ξ values

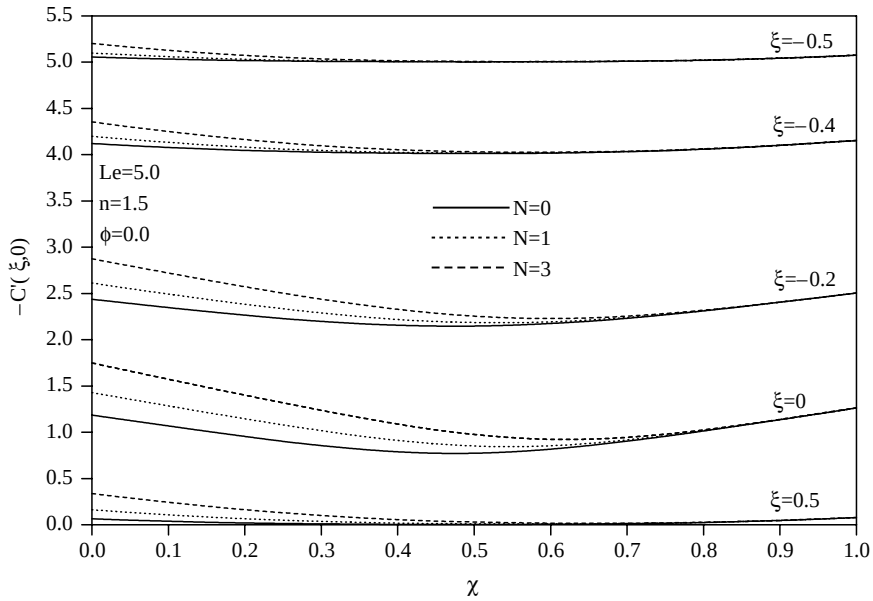

Figure 12.
Effects of N and χ on local Sherwood number for $n = 1.5$ and different ξ values

increases in the value of N have the tendency to increase the buoyancy effect causing more induced flow along the surface in the vertical direction. However, both the temperature and concentration along with their boundary layers decrease. This causes the negative wall slope of the temperature and concentration profiles to increase yielding enhancements in both the local Nusselt and Sherwood numbers. Also, it is noted that as the transformed suction or injection parameter ξ increases for fixed values of $N > 0$ and $\chi \neq 1$, the temperature and concentration as well as their boundary layers increase. This produces higher flow velocities due to increases in the buoyancy effects. As a result of increasing the value of ξ, the local Nusselt and Sherwood numbers increase. From the definition of χ, it is seen that increases in the value of the parameter Ra_x/Pe_x causes the mixed convection parameter χ to decrease. Thus, small values of Ra_x/Pe_x correspond to values of χ close to unity which indicate almost pure forced convection regime. On the other hand, high values of Ra_x/Pe_x correspond to values of χ close to zero which indicate almost pure free convection regime. Furthermore, moderate values of Ra_x/Pe_x represent values of χ between 0 and 1 which correspond to the mixed convection regime. For the forced convection limit ($\chi = 1$) it is clear from equation (15) that the velocity in the boundary layer f' is uniform irregardless of the value of n. However, for smaller values of χ (higher values of Ra_x/Pe_x) at a fixed value of N and $n = 1.0$, the buoyancy effect increases. As this occurs, the fluid velocity close to the wall increases for values of $\chi \leq 0.5$ due to the buoyancy effect which becomes maximum for $\chi = 0$ (free convection limit). This decrease and increase in the fluid velocity f' as χ is decreased from unity to zero is accompanied by a respective increase and a decrease in the fluid temperature and concentration. As a result, the local Nusselt and Sherwood numbers tend to decrease and then increase as χ is increased from 0 to unity forming slight dips close to $\chi = 0.4$ for $n = 1$ (Figures 9 and 10) and $\chi = 0.5$ for $n = 1.5$ (Figures 11 and 12) for almost all

values of ξ and N considered. However, for $n = 0.5$ and $N \leq 1.0$, the local Nusselt and Sherwood numbers are predicted to increase as χ is increased from 0 to unity. On the other hand, for $N = 3$, the added buoyancy due to concentration gradient causes a different trend in which the local Nusselt and Sherwood numbers increase with increasing values of χ. Furthermore, by comparison of Figures 7-12, one can easily conclude that the local Nusselt and Sherwood numbers decrease as the power-law fluid index n increases. It is also observed that while the local Nusselt and Sherwood numbers change in the whole range of free and mixed convection regime, they remain constant for the forced-convection regime. This is obvious since for $\chi = 1$ and fixed values of Le and ϕ, the equations are the same and do not depend on n and N. All of the above trends are clearly shown in Figures 7-12.

Figure 13 shows the effects of the heat generation or absorption coefficient ϕ on the temperature profiles for different values of ξ. The presence of a heat generation source in the flow represented by positive values of ϕ enhances the thermal state of the fluid causing its temperature to increase. On the contrary, the presence of a heat absorption sink in the flow represented by negative values of ϕ reduces the fluid temperature. These behaviors are clearly seen from Figure 13. Also, it should be noted that for the case of heat generation ($\phi \geq 0.5$ and $\xi \geq 1$) the maximum fluid temperature does not occur at the wall but rather in the fluid layer adjacent to the wall. The curve associated with $\phi = 0.5$ and $\xi = 2$ is not plotted because the peak value lies outside the scale of Figure 13.

The effect of the heat generation or absorption coefficient ϕ on the local Nusselt number $[Nu_x/(Pe_x^{1/2} + Ra_x^{1/2}) = -\theta'(\xi, 0)]$ for different values of n (0.5, 1.0, 1.5) in the range $-2 \leq \xi \leq 2$ is shown in Figure 14. As mentioned above, the presence of a heat generation effects in the flow increases the fluid temperature to increase. This, in turn, increases the thermal buoyancy effect which produces higher induced flow. On the

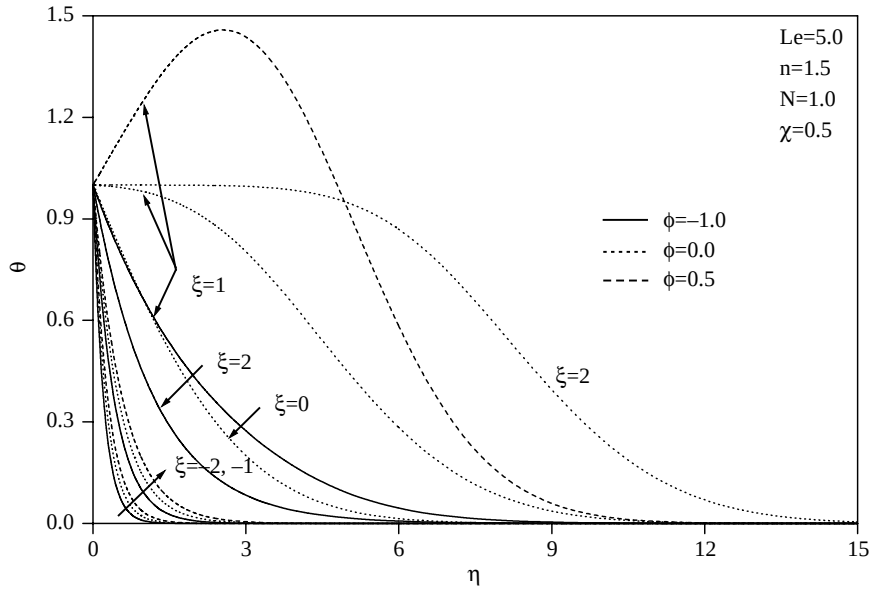

Figure 13.
Temperature profiles for different values of ξ and ϕ ($n = 1.5$)

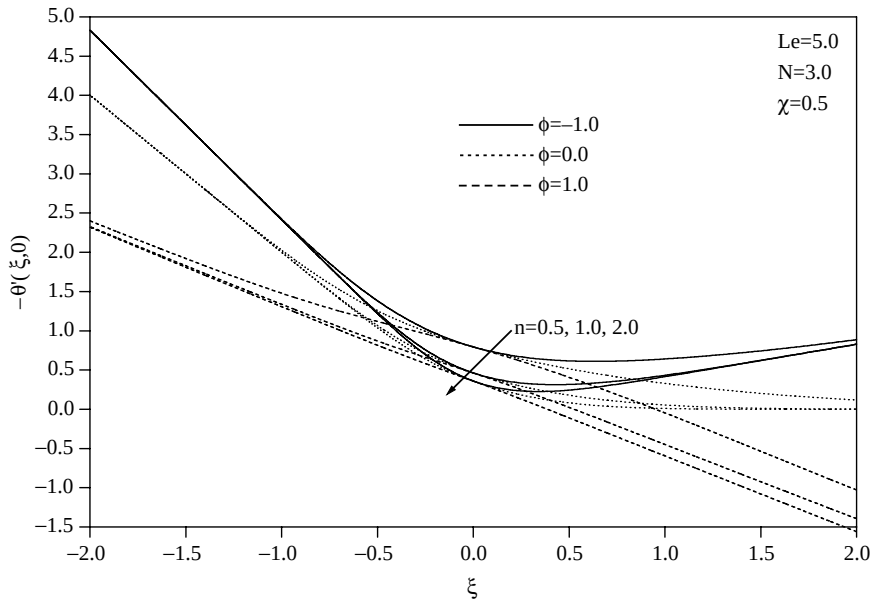

Figure 14.
Variation of local Nusselt number with ξ for different values of n and ϕ

contrary, the presence of a heat absorption effects in the flow reduces the fluid temperature which, in turn, decreases the induced flow due to thermal buoyancy effects. Thus, the wall slope of the temperature profile increases as ϕ increases causing the local Nusselt number which is directly proportional to $-\theta'(\xi, 0)$ to decrease for all values of ξ except $\xi = 0$ since ϕ does not appear in equation (16) at $\xi = 0$. As seen from Figure 13, for the heat generation case ($\phi \geq 0.5$ and $\xi \geq 1$), the maximum fluid temperature does not occur at the wall but rather in the fluid layer adjacent to the surface for some values of $\xi > 0$. This causes the slope of the temperature profile at the wall $\theta'(\xi, 0)$ to become positive and thus, the local Nusselt number is negative. All these behaviors are clear from Figure 14. Also, it is observed that as n increases, the local Nusselt number decreases and that the amount of reduction depends on the values of ξ and ϕ.

Figure 15 shows the effect of increasing the Lewis number Le on the concentration profile for different values of ξ. In general, increases in the value of the Lewis number result in decreasing the concentration distribution within the boundary layer. However, it is observed that for values of $\xi > 0$ as Le increases, the concentration level close to the surface increases while its distribution within the boundary layer away from the surface decreases. This behavior is shown in Figure 15.

Figure 16 shows the influence of the Lewis number Le on the local Sherwood number in the whole mixed convection range $0 \leq \chi \leq 1$ for values of $\xi > 0$. Increasing the values of the Lewis number in the range $0 \leq \xi \leq 0.2$ results in increasing the concentration level close to the wall while decreasing its distribution within the boundary layer away from the surface. This causes the local Sherwood number to increase. However, in the range $\xi > 0.2$, increasing Le reduces the concentration everywhere in the boundary layer causing the local Sherwood number to decrease. These behaviors are shown clearly in Figure 16.

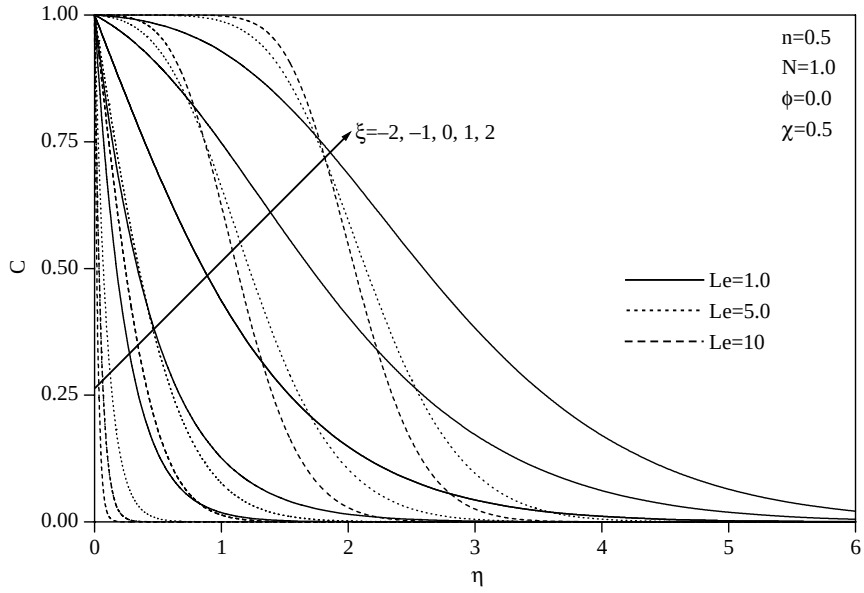

Figure 15.
Concentration profiles for different values of ξ and Le ($n = 0.5$)

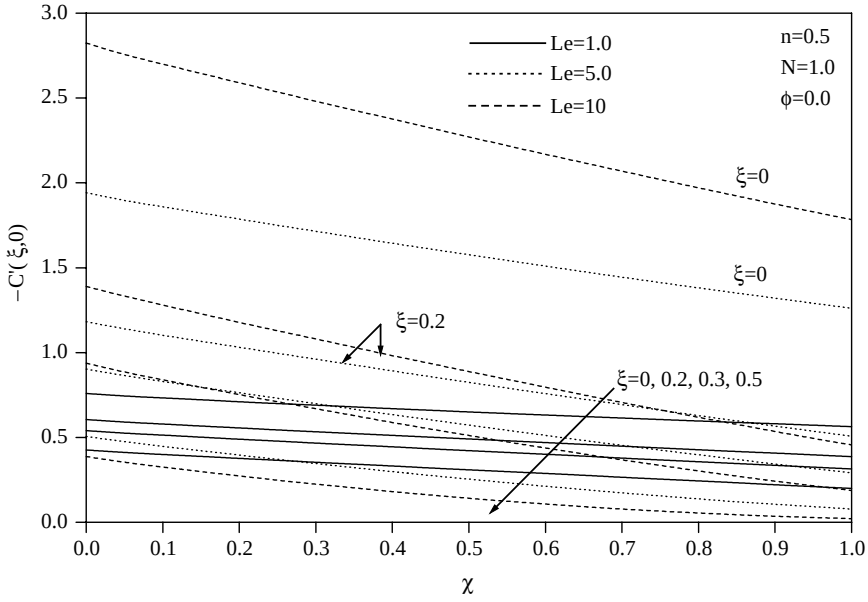

Figure 16.
Effects of Le and χ on local Sherwood number for $n = 0.5$ and different ξ values

Conclusions

This study considered heat and mass transfer by mixed convection from a vertical permeable surface embedded in a porous medium for a non-Newtonian power-law fluid in the presence of temperature-dependent heat generation or absorption effects.

A single parameter for the entire range of free-forced-mixed convection regime was employed. The obtained non-similar differential equations were solved numerically by an efficient implicit finite-difference method. The results focused on the effects of the buoyancy ratio, power-law fluid index, mixed convection parameter, suction or injection parameter, heat generation or absorption parameter, and the Lewis number on the local Nusselt and Sherwood numbers. It was found that as the buoyancy ratio was increased, both the local Nusselt and Sherwood numbers increased in the whole range of free and mixed convection regime while they remained constant for the forced-convection regime. However, they decreased and then increased forming dips as the mixed-convection parameter was increased from the free-convection limit to the forced-convection limit for both Newtonian and dilatant fluid situations. On the other hand, in general, for pseudo-plastic fluids the local Nusselt and Sherwood numbers decreased with increasing values of the mixed-convection parameter for smaller values of the buoyancy ratio (less than or equal unity) while they increase with it for larger values of the buoyancy ratio. Furthermore, it was concluded that the local Nusselt and Sherwood numbers decreased as the power-law fluid index was increased. The effect of heat generation was found to decrease the local Nusselt number while the opposite was predicted for heat absorption conditions. In general, the local Sherwood number was increased with increases in the Lewis number.

References

Acharya, S. and Goldstein, R.J. (1985), "Natural convection in an externally heated vertical or inclined box containing internal energy sources", *J. Heat Transfer*, Vol. 107, pp. 855-66.

Blottner, F.G. (1970), "Finite-difference methods of solution of the boundary-layer equations", *AIAA Journal*, Vol. 8, pp. 193-205.

Chen, H.T. and Chen, C.K. (1988), "Free convection of non-Newtonian fluids along a vertical plate embedded in a porous medium", *Trans. ASME, J. Heat Transfer*, Vol. 110, pp. 257-60.

Cheng, P. (1977), "The influence of lateral mass flux on free convection boundary layers in a saturated porous medium", *Int. J. Heat Mass Transfer*, Vol. 20, pp. 201-6.

Cheng, P. and Minkowycz, W.J. (1977), "Free convection about a vertical flat plate embedded in a porous medium with application to heat transfer from a dike", *J. of Geophys. Res.*, Vol. 82, pp. 2040-4.

Christopher, R.H. and Middleman, S. (1965), "Power-law flow through a packed tube", *I & EC Fundamentals*, Vol. 4, pp. 422-6.

Dharmadhikari, R.V. and Kale, D.D. (1985), "Flow of non-Newtonian fluids through porous media", *Chemical Eng. Sci.*, Vol. 40, pp. 527-9.

Gorla, R.S.R. and Kumari, M. (1998), "Nonsimilar solutions for mixed convection in non-Newtonian fluids along a vertical plate in a porous medium", *Transport in Porous Media*, Vol. 33, pp. 295-307.

Gorla, R.S.R., Slaouti, A. and Takhar, H.S. (1997a), "Mixed convection in non-Newtonian fluids along a vertical plate in porous media with surface mass transfer", *International Journal of Numerical Methods for Heat & Fluid Flow*, Vol. 7, pp. 598-608.

Gorla, R.S.R., Shanmugam, K. and Kumari, M. (1997b), "Nonsimilar solutions for mixed convection in non-Newtonian fluids along horizontal surfaces in porous media", *Transport in Porous Media*, Vol. 28, pp. 319-34.

Gorla, R.S.R., Shanmugam, K. and Kumari, M. (1998), "Mixed convection in non-Newtonian fluids along nonisothermal horizontal surfaces in porous media", *Heat and Mass Transfer*, Vol. 33, pp. 281-6.

Hooper, W.B., Chen, T.S. and Armaly, B.F. (1993), "Mixed convection from a vertical plate in porous media with surface injection or suction", *Numer. Heat Transfer*, Vol. 25, pp. 317-29.

Hsieh, J.C., Chen, T.S. and Armaly, B.F. (1993), "Non-similarity solutions for mixed convection from vertical surfaces in a porous medium", *Int. J. Heat Mass Transfer*, Vol. 36, pp. 1485-93.

Jumah, R.Y. and Mujumdar, A.S. (2000), "Free convection heat and mass transfer of non-Newtonian power law fluids with yield stress from a vertical flat plate in saturated porous media", *Int. Commun. Heat Mass Transfer*, Vol. 27, pp. 485-94.

Kumari, M., Gorla, R.S.R. and Byrd, L. (1997), "Mixed convection in non-Newtonian fluids along a horizontal plate in a porous medium", *Trans. ASME, J. Energy Resour. Technol.*, Vol. 119, pp. 34-7.

Lai, F.C. (1991), "Coupled heat and mass transfer by mixed convection from a vertical plate in a saturated porous medium", *Int. Commun. Heat Mass Transfer*, Vol. 18, pp. 93-106.

Lai, F.C. and Kulacki, F.A. (1990a), "The influence of surface mass flux on mixed convection over horizontal plates in saturated porous media", *Int. J. Heat Mass Transfer*, Vol. 33, pp. 576-9.

Lai, F.C. and Kulacki, F.A. (1990b), "The influence of lateral mass flux on mixed convection over inclined surfaces in saturated porous media", *J. Heat Transfer*, Vol. 112, pp. 515-8.

Mehta, K.N. and Rao, K.N. (1994a), "Buoyancy-induced flow of non-Newtonian fluids over a non-isothermal horizontal plate embedded in a porous medium", *Int. J. Eng. Sci.*, Vol. 32, pp. 521-5.

Mehta, K.N. and Rao, K.N. (1994b), "Buoyancy-induced flow of non-Newtonian fluids in a porous medium past a vertical plate with nonuniform surface heat flux", *Int. J. Eng. Sci.*, Vol. 32, pp. 297-302.

Minkowycz, W.J., Cheng, P. and Moalem, F. (1985), "The effect of surface mass transfer on buoyancy-induced Darcian flow adjacent to a horizontal heated surface", *Int. Commun. Heat Mass Transfer*, Vol. 12, pp. 55-65.

Nakayama, A. and Koyama, H.A. (1987), "General similarity transformation for free, forced and mixed convection in Darcy and non-Darcy porous media", *J. Heat Transfer*, Vol. 109, pp. 1041-5.

Ranganathan, P. and Viskanta, R. (1984), "Mixed convection boundary layer flow along a vertical surface in a porous medium", *Numerical Heat Transfer*, Vol. 7, pp. 305-17.

Vajravelu, K. and Nayfeh, J. (1992), "Hydromagnetic convection at a cone and a wedge", *Int. Commun. Heat Mass Transfer*, Vol. 19, pp. 701-10.

Corresponding author
Ali J. Chamkha can be contacted at: achamkha@yahoo.com

To purchase reprints of this article please e-mail: **reprints@emeraldinsight.com**
Or visit our web site for further details: **www.emeraldinsight.com/reprints**